Research Article | Vol. 27, No. 8 | 15 Apr 2019 | OPTICS EXPRESS 11292
Optics EXPRESS

# Optimum quantum resource distribution for phase measurement and quantum information tapping in a dual-beam SU(1,1) interferometer

YUHONG LIU,[1] NAN HUO,[1] JIAMIN LI,[1] LIANG CUI,[1] XIAOYING LI,[1,*] AND ZHEYU JEFF OU[1,2,3]

[1] *College of Precision Instrument and Opto-Electronics Engineering, Key Laboratory of Opto-Electronics Information Technology, Ministry of Education, Tianjin University, Tianjin 300072, China*
[2] *Department of Physics, Indiana University-Purdue University Indianapolis, Indianapolis, IN 46202, USA*
[3] *zheyuou@tju.edu.cn*
[*] *xiaoyingli@tju.edu.cn*

**Abstract:** Quantum entanglement is a resource in quantum metrology that can be distributed to two conjugate physical quantities for the enhancement of their measurement sensitivity. This is demonstrated in the joint measurement of phase and amplitude modulation signals in quantum dense metrology schemes. We can also devote all the quantum resource to phase measurement only, leading to the optimum sensitivity enhancement. In this paper, we experimentally implement a dual-beam sensing scheme in an SU(1,1) interferometer for the optimum quantum enhancement of phase measurement sensitivity. We demonstrate a 3.9-dB improvement in signal-to-noise ratio over the optimum classical method, and this is 3-dB better than the traditional single-beam scheme. Furthermore, such a scheme also realizes a quantum optical tap of quantum entangled fields and has the full advantages of an SU(1,1) interferometer, such as detection loss tolerance, making it more suitable for practical applications in quantum metrology and quantum information.



## 1. Introduction

Phase measurement sensitivity has been a topic of constant interest ever since optical interferometry technique was invented more than one hundred years ago [1]. The employment of quantum states of light in interferometry has now pushed the measurement sensitivity to a new limit, beyond what is allowed with classical coherent sources of light [2,3]. Squeezed states, because of the property of quantum noise reduction, are usually applied to a traditional interferometer for sensitivity enhancement in phase measurement [2,4,5]. Quantum entanglement, as a quantum resource, can also be applied to enhance phase measurement sensitivity by quantum noise cancelation via quantum correlation [6,7].

Recently, SU(1,1) interferometer (SUI) was demonstrated to exhibit sensitivity enhancement in phase measurement [8–21] and in the meantime possesses detection loss tolerance property [11,13,15], which is a huge advantage over the squeezed state schemes. Although the hardware of the new interferometer changes from beam splitters to parametric amplifiers, the underlining physics is still quantum noise cancelation through quantum entanglement [14,22–24], similar to works in [6]. However, it was shown in [24] that these quantum entanglement-based schemes can only give rise to half the sensitivity enhancement in phase measurement as compared to the squeezed state schemes with the same power strength defined through the gain of the parametric processes for their generations. The study discovered that these schemes are also able to increase the sensitivity of the amplitude measurement concurrently with the phase measurement in the name of "quantum dense metrology" [24–27]. Therefore, the quantum resource of entanglement is split between phase and amplitude measurement.

To increase the sensitivity enhancement factor, on par with the squeezed state schemes, we need

#346600 https://doi.org/10.1364/OE.27.011292
Journal © 2019 Received 11 Oct 2018; revised 28 Mar 2019; accepted 29 Mar 2019; published 9 Apr 2019

Optics EXPRESS

to devote all the quantum resource to phase measurement only. In this paper, we experimentally implement a variation of the SUI which employs both the signal and the idler beams to probe a common phase shift. We find this dual beam sensing scheme can double the sensitivity of the original single-beam sensing scheme, making full use of the quantum resource of entanglement for phase measurement.

## 2. Theory

Traditionally, phase is measured by an interferometer where one of its arms probes the phase change while the other serves as a reference. This is precisely the principle of homodyne detection shown in Fig. 1(a). When a probe beam in coherent state $|\alpha\rangle$ with $\alpha = |\alpha|e^{i\phi_0}$ propagates through a phase modulator (PM) and carries the weak phase modulation signal $\delta$, the field to be measured is then written as $\hat{a} = \hat{a}_0 e^{i\delta} \approx \hat{a}_0 (1 + i\delta)$, where $\hat{a}_0$ is the annihilation operator for probe beam and $\phi_0$ is the initial phase of probe. A direct homodyne detection of the modulated beam measures the quadrature amplitude $\hat{X}(\theta) = \hat{a}e^{-i\theta} + \hat{a}^\dagger e^{i\theta}$ , where $\theta$ is the difference between the phase of probe field and the local oscillator. Defining $\hat{X} = \hat{X}(0) = \hat{a} + \hat{a}^\dagger$ and $\hat{Y} = \hat{X}(\pi/2) = i\left(\hat{a}^\dagger - \hat{a}\right)$ as two conjugate observables, we can obtain the power of modulation signal: $\left\langle \hat{Y} \right\rangle^2 = 4|\alpha|^2 \delta^2$ when the quadrature amplitude $\hat{Y}$ is measured. Since the noise of the coherent state is $\left\langle \Delta^2 \hat{X}(\theta) \right\rangle = 1$ , it is straightforward to show that the signal-to-noise ratio (SNR) of phase modulation signal is:

$$SNR_{HD} = 4|\alpha|^2\delta^2 = 4I_{ps}\delta^2, \tag{1}$$

where $I_{ps} \equiv |\alpha|^2$ with $\alpha$ denoting a complex number is the intensity of the phase sensing probe beam. Since the ideal homodyne detection is free of classical noise, its sensitivity is only limited by the quantum noise in the probe field. Equation (1) gives the optimum SNR for a probe field based on classical light source such as a laser beam in coherent state. It should be mentioned that a traditional Michelson or Mach-Zehnder interferometer with balanced intensities at two arms and work at dark fringe only produces half the classical optimum SNR in Eq. (1) [11, 28, 29]. This is because for these traditional interferometers, the power of modulated signal is equally distributed to two outputs, while the measurement noise is still the vacuum noise (the same as the noise of coherent states). In the following, we will compare all our results of dual-beam sensing schemes to the optimum classical SNR in Eq. (1).

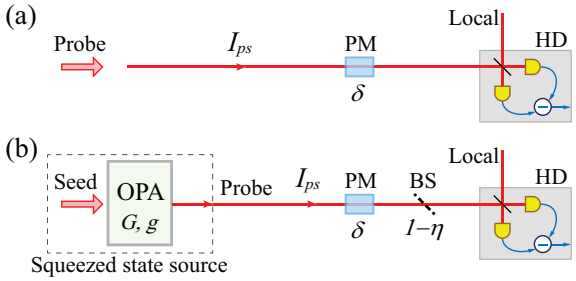


Fig. 1. Typical phase measurement by homodyne detection with (a) classical coherent state and (b) coherent squeezed state. OPA, optical parametric amplifier; PM, phase modulator; HD, homodyne detection; $I_{ps}$, phase sensing field intensity; BS, beam splitter with transmission efficiency of $1 - \eta$ is used to model non-ideal detection efficiency.

With a quantum light source such as a coherent squeezed state as the probe (see Fig. 1(b)), quantum noise can be reduced and the SNR can be improved to

$$SNR_{SQ} = 4|\alpha|^2\delta^2/S = 4I_{ps}\delta^2(G+g)^2 \tag{2}$$

Optics EXPRESS

by a factor of $1/S \equiv (G+g)^2$ as compared to the classical optimum SNR in Eq. (1), where the parameter $S$ is the so-called squeezing degree. The amplitude gains G and g, satisfying the relation $G^2 - g^2 = 1$, can be expressed as $G = \cosh(r)$ and $g = \sinh(r)$, where the parameter $r$ denotes the nonlinear coupling coefficient of the parametric process in optical parametric amplifier (OPA) [9, 30]. However, transmission and detection losses introduce vacuum noise and degrade the enhancement factor to

$$1/S_1 = 1/[S + \eta/(1-\eta)] \tag{3}$$

with $\eta$ denoting the overall loss (modeled as a beam splitter (BS) with transmission efficiency $1-\eta$ in Fig. 1(b)).

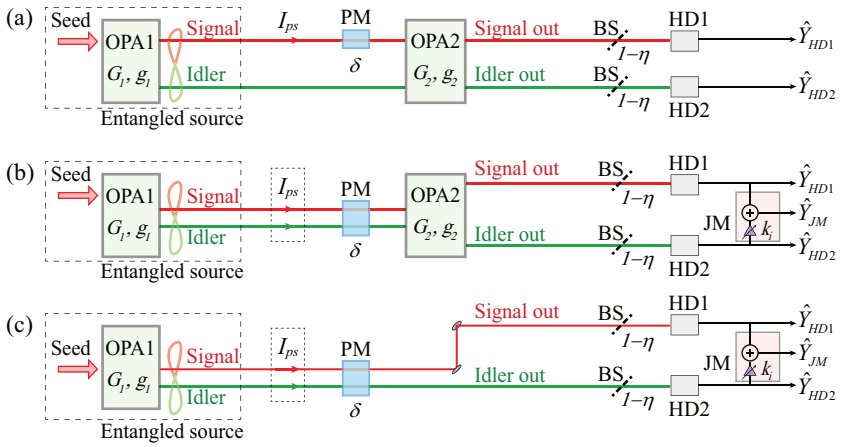


Fig. 2. Phase measurement schemes with entangled source generated from an optical parametric amplifier (OPA1). (a), single-beam sensing SU(1,1) interferometer; (b), dual-beam sensing SU(1,1) interferometer; (c), direct joint measurement scheme. PM, phase modulator; HD1-2, homodyne detection; $I_{ps}$, phase sensing field intensity. BS, beam splitter with transmission efficiency of $1-\eta$ is used to model non-ideal detection efficiency; $k_i$, electronic variable gain; JM, joint measurement.

Quantum enhanced phase measurement can also be achieved with SUI, which utilizes parametric amplifiers for wave splitting and superposition, as shown in Fig. 2(a). Variations of SUI include the scheme with the second parametric amplifier replaced by a beam splitter [22] and a truncated scheme where homodyne measurements are performed directly on the modulated beam, and the resulting photo-currents are added or subtracted for quantum noise cancellation [14, 16, 23]. It was shown in [24] that all these previous used SUI schemes have an optimum phase measurement sensitivity characterized by the SNR as

$$SNR_{SUI} = 2I_{ps}\delta^2(G_1 + g_1)^2. \tag{4}$$

For the scheme in Fig. 2(a), Eq. (4) is obtained for $G_2 \gg G_1$ and locking the OPA2 at the de-amplification condition, where $G_1$ and $G_2$ are the amplitude gains for OPA1 and OPA2, respectively. The de-amplification condition is realized by setting the phase relation [31]:

$$\phi_{SUI} = \phi_s + \phi_i - 2\phi_p \tag{5}$$

at $\phi_{SUI} = \pi$, where $\phi_s$,$\phi_i$ and $\phi_p$ are the phase of signal, idler and pump field injected into OPA2 respectively. This, however, has an improvement factor of $1/S_2 = (G_1 + g_1)^2/2$, which is only half of that given in Eq. (2) with equivalent $G_1 = G$.

Optics EXPRESS

We now explore the reason for the difference between the two results in Eqs. (2) and (4). It was demonstrated recently [24, 27] that the scheme in Fig. 2(a) can also be used to measure amplitude modulation on the probe beam at the other output port (HD2) of the second amplifier of the SUI with the same SNR given in Eq. (4). Since the phase measurement and the amplitude measurement are performed at different ports of the OPA2, they can be done simultaneously, sharing the same resource of quantum entanglement generated by OPA1 [24]. Because of this, the quantum resource is split between the phase and amplitude measurement, reducing the quantum enhancement effect by half for each measurement.

Realizing this difference, we now construct a variation of SUI to place all the quantum resource to phase measurement. Different from Fig. 2(a), in which the signal beam between two OPAs functions as the probe, our new measurement scheme involves both correlated signal and idler fields for probing the phase change, as shown in Fig. 2(b). A quick comparison of the new scheme with the traditional interferometer may lead to the concern that the phase signal would be cancelled in phase difference, a phenomenon known as "common mode rejection" in traditional interferometer. In traditional interferometers, the interference fringe is determined by the phase difference $\phi_1 - \phi_2$ between two arms of interferometer. When phase modulation is applied on both arms, the modulation signal at the output port will be cancelled out by the subtraction process. Fortunately, the working principle of SUI is totally different from that of a traditional interferometer [10, 32]. The OPA2 in SUI is a phase sensitive amplifier and its output intensity is decided by the phase relation in Eq. (5). Hence, for SUI locked at the de-amplification condition, its output depends on the sum of the phase of the two arms rather than the difference for a traditional interferometer.

Equation (4) shows that the quantum enhanced measurement is originated from the two entangled outputs of OPA1 that have the quantum correlation [33]: $\left\langle \Delta(\hat{X}_1 - \hat{X}_2)^2 \right\rangle /2 < 1$ and $\left\langle \Delta(\hat{Y}_1 + \hat{Y}_2)^2 \right\rangle /2 < 1$, where $\hat{X}_{1(2)}$ and $\hat{Y}_{1(2)}$ are the two conjugate quadrature amplitudes of signal (idler) field out of OPA1. When the SUI is working at the dark fringe, the noise at each output is reduced due to quantum noise cancellation occurred in OPA2 [34]. If the dual beams co-propagate through a PM, the phase signal carried by each beam will add up coherently at each output of SUI because of the negative correlation between $\hat{Y}_1$ and $\hat{Y}_2$. Therefore, the detected power of modulation signal $\delta$ will be quadrupled as compared to the single beam sensing SUI scheme in Fig. 2(a), but $I_{ps}$ will also double because of the dual-beam probing (under the condition of $G_1 \gg 1, G_1 \approx g_1$). As a result, there is an increase of the SNR by a factor of 2, recovering the SNR in Eq. (2). The SNR of phase signal measured by homodyne detection (HD) at each output of SUI is given by:

$$\begin{aligned} SNR_{HD1} &= \frac{4(G_1G_2 + g_1g_2)^2|\alpha|^2\delta^2}{(G_2G_1 - g_2g_1)^2 + (G_2g_1 - g_2G_1)^2} \\ SNR_{HD2} &= \frac{4(G_1g_2 + g_1G_2)^2|\alpha|^2\delta^2}{(G_2G_1 - g_2g_1)^2 + (G_2g_1 - g_2G_1)^2} \end{aligned} \tag{6}$$

which reach the optimum value when $G_2 \to \infty$:

$$\begin{aligned} SNR_{HD1}^{(op)} = SNR_{HD2}^{(op)} &= 2(G_1 + g_1)^4 I_{ps}\delta^2/(G_1^2 + g_1^2) \\ &\approx 4(G_1 + g_1)^2 I_{ps}\delta^2 \ \text{ for } \ g_1 \gg 1 \end{aligned} \tag{7}$$

where $I_{ps} \equiv (G_1^2 + g_1^2)|\alpha|^2$ ($|\alpha|^2 \gg 1$) is the phase sensing probe intensity.

The results in Eq. (7) are in exactly the same form as Eq. (2), which is twice of that in Eq. (4) for single beam sensing scheme. On the other hand, the "common mode rejection effect" does apply to amplitude modulation. If an amplitude modulation signal $\epsilon$ is encoded by passing both the signal and idler beams through an amplitude modulator, the signal size measured at one output of SUI ($4\,(G_1g_2 - g_1G_2)^2\, I_{ps}\epsilon^2/(G_1^2 + g_1^2)$) is much less than that of phase signal

$(4\,(G_1G_2 + g_1g_2)^2\, I_{ps}\delta^2/(G_1^2 + g_1^2))$ because of the positive correlation relation between the quadrature amplitudes of signal and idler inputs ($\hat{X}_1$ and $\hat{X}_2$) for OPA2 [24]. So, this scheme cannot be used for quantum enhanced amplitude measurement at all. From this analysis, we find all the quantum resource is used for phase measurement alone and this scheme recovers the enhancement factor lost due to quantum resource sharing in single beam sensing scheme [24, 27].

It should be noted that in addition to the homodyne detection that realize measurement on $\hat{Y}_{HD1}$ or $\hat{Y}_{HD2}$ at each output of OPA2, joint measurement

$$\hat{Y}_{JM} = \hat{Y}_{HD1} + k_i\hat{Y}_{HD2} \tag{8}$$

can be performed by adding up the photo-currents out of HD1 and HD2, as shown in Fig. 2(b), where $k_i$ is a variable gain parameter for maximizing the SNR of $\hat{Y}_{JM}$. Although optimum performance of SUI can be achieved by the direct homodyne measurement of $\hat{Y}_{HD1}$ or $\hat{Y}_{HD2}$ at the signal or idler output of SUI when $G_2 \to \infty, G_1 \gg 1$, it is shown that the joint measurement can give rise to the optimum quantum enhancement in Eq. (7) by properly adjusting the electronic gain parameter $k_i$ in the joint measurement circuit even at finite gains of $G_2$ [34].

It is worth noting that when the gain coefficient of OPA2 is $G_2 = 1$ (or $g_2 = 0$), OPA2 function as an ideal transmission media for signal and idler beams. In this case, Fig. 2(b) is equivalent to Fig. 2(c) when the joint measurement is performed to extract the phase information encoded on dual beams. For Fig. 2(c), it is straightforward to show that the SNR in the measurement of the joint quantity $Y_{JM}$ is the same as that given in Eq. (2) with equivalent $G = G_1$ when the gain parameter $k_i$ in Eq. (8) takes the optimized value of $k_i = 1$ [16, 24]. However, the scheme shown in Fig. 2(c) is sensitive to detection losses, and the dependence of the enhancement degradation on loss is exactly the same as the squeezed state scheme in Fig. 1(b) discussed earlier (see Eq. (3)). This similarity between the two schemes is because the co-propagate signal and idler entangled fields in Fig. 2(c) are nearly degenerate, while the squeezed state in Fig. 1(b) is indeed formed by two degenerated fields out of OPA. When both the entangled signal and idler fields from OPA1 are used to probe the phase shift introduced by PM, the phase information carried by the dual beams is similar to that by squeezed state as long as the gain of OPA in the two cases is the same. For the SUIs in Figs. 2(a) and 2(b), however, it is another story [24]. With the presence detection losses (denoted as BS with transmission $1 - \eta$ before detection), the improvement factor changes to

$$1/S_3 \approx 1/[S + \eta/2G_2^2(1 - \eta)] \tag{9}$$

for the result measured by HD1/HD2 at one output of OPA2, or

$$1/S_3 \approx 1/[S + \eta/4G_2^2(1 - \eta)] \tag{10}$$

for the result jointly measured by two HDs, and we approximately have $1/S_3 \approx 1/S$ when $G_2 \gg G_1$ and $G_2 \approx g_2$. So, the scheme of SUI using OPA2 to coherently combine the entangled signal and idler fields is tolerant to detection losses. This is because the output noise of OPA2 is much larger than vacuum noise so that the vacuum noise coupled in through loss channel is negligible.

Another interesting application of the dual-beam sensing scheme in Fig. 2(b) is the realization of a quantum information tap [35, 36]. In this case, OPA2 is regarded as the information splitter for the input, which is the entangled fields from OPA1 with weak phase signal encoded by PM. The input SNR corresponding to the direct joint measurement result in Fig. 2(c) is:

$$SNR_{in} = 4I_{ps}\delta^2(G_1 + g_1)^2, \tag{11}$$

for lossless case. With output SNRs at the two output of OPA2 given in Eq. (7), we have the

Optics EXPRESS

optimum transfer coefficients as

$$T_{HD1,HD2} \equiv \frac{SNR^{(op)}_{HD1,HD2}}{SNR_{in}} = \frac{(G_1+g_1)^2}{2(G_1^2+g_1^2)} \approx 1 \text{ for } g_1 \gg 1, \tag{12}$$

which means that the signal encoded in the entangled fields can be split into two by the amplifier without adding noise in the ideal case of $g_1 \gg 1$. In general, we have $T_{HD1} + T_{HD2} = (G_1+g_1)^2/(G_1^2+g_1^2) > 1$, satisfying the condition for quantum optical tapping [35].

## 3. Experiment setup

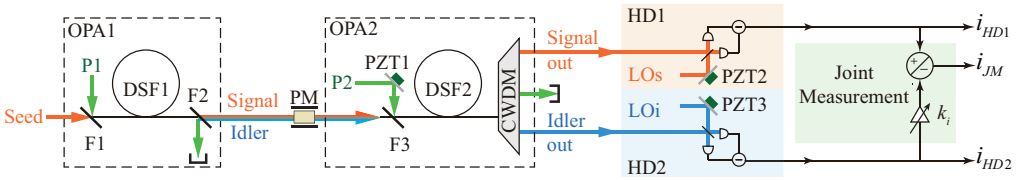


Fig. 3. Experiment setup. OPA1-2, optical parametric amplifiers; P1-2, pump for OPA1-2; F1-3, band-reflection filter centering at 1550 nm; DSF1-2. dispersion shifted fiber; PM, phase modulator; CWDM, coarse wavelength division multiplexer; HD1-2, homodyne detectors; LOs(LOi), local oscillator for signal (idler) field; PZT1-3, piezo-electric transducer; $k_i$, electronic variable gain; JM, joint measurement.

We implement experimentally the dual-beam schemes in Figs. 2(b) and 2(c), in which the OPAs are realized by using fiber-based OPAs. The experimental setup for measuring the weak phase modulation by using the dual-beam sensing SUI is shown in Fig. 3. The nonlinear media for OPA1 and OPA2 are two pieces of identical dispersion shifted fibers (DSF1 and DSF2). The length and zero dispersion wavelength of each DSF are about 150 m and 1548.5 nm, respectively. The pump for each OPA, P1/P2, is a mode locked pulse train. Each pulsed pump with full width at half maximum (FWHM) of 0.4 nm is centered at 1549 nm to ensure the phase matching of four wave mixing (FWM) parametric process is satisfied in DSF [37]. OPA1 generates the entangled signal and idler beams [33,38]. When the strong pump P1 and weak seed injection centering at 1533 nm are combined by a wavelength division multiplexer (WDM) filter (F1) and simultaneously launched into DSF1, we obtain the amplified signal beam and generated idler beam via FWM. By passing the output of OPA1 through a WDM filter (F2), we isolate the residual power of pump P1 and select out the entangled signal and idler beams, which are centering at 1533 and 1566 nm, respectively, and co-propagate in space. The weak phase signal is encoded by propagating both the signal and idler beams through a phase modulator modulated at the frequencies of 1.56 MHz. The encoded dual beams are combined with the pump P2 and simultaneously launched into DSF2 for signal amplification and noise suppression. At the output of OPA2, we exploit a 2-channel course wavelength division multiplexer (CWDM) to isolate the pump P2 and to select the signal and idler fields with high efficiency. For the two channels of CWDMs, the isolation degrees to the pump are greater than 40 dB. At the two outputs of OPA2, the signal and idler fields are respectively measured by the homodyne detection systems HD1 and HD2. The local oscillator (LOs/LOi) of each homodyne detection HD1/HD2 is properly locked to measure the quadrature amplitude $\hat{Y}_{HD1/HD2}$ at signal/idler output port. When the joint measurement is performed, we mix the photo-currents $i_{HD1}$ and $i_{HD2}$ of HD1 and HD2, respectively, with a mixer to obtain $i_{JM} = i_{HD1} + k_i i_{HD2}$, where the output of HD2 is adjusted by the electrical gain $k_i$ to optimize the measured SNR. The power spectrum of measurement

Optics EXPRESS

result is analyzed by sending the photon-currents directly out of each individual homodyne detector and joint measurement of HD1 and HD2, which are $i_{HD1}$, $i_{HD2}$ and $i_{JM}$, into a data acquisition system (DAQ).

To ensure the phase signal encoded on the dual-beam can be measured at each output of SUI with high SNR, the power gain of OPA2 should be much higher than that of OPA1. During the measurement, the powers of P1 and P2 are 2 mW and 4 mW, respectively. In this condition, the power gains of OPA1 and OPA2 are about 2.5 and 12, respectively. Moreover, to obtain the best noise cancelation effect, OPA2 is operated at the de-amplification condition by locking the phase relative in Eq. (5) to $\phi_{SUI} = \pi$. This is realized by controlling the phase of P2 with the piezoelectric transducer (PZT1).

To clearly demonstrate the quantum enhancement, we need to compare the SNR measured by the dual-beam sensing SUI with that obtained by classical method. The classical method, corresponding to the homodyne detection in Fig. 1(a), is realized by setting the powers of two pumps (P1 and P2) to zero so that the two DSFs simply function as transmission media. On the other hand, to illustrate the loss tolerance feature, we should compare the measurement results of dual-beam sensing SUI with that obtained by using entanglement out of OPA1 (the pump of OPA1 is on, while that of OPA2 is off) and by directly performing joint measurement, which is equivalent to the scheme in Fig. 2(c). It is worth noting that in each case, the probe beam intensity $I_{ps}$ is adjusted to be the same for fair comparison. The measurement results presented in Sec. 4 are obtained for $I_{ps} = 200$ pW.

In the experiment, the two pumps (P1 and P2) are obtained by carving the output of a femto-second laser with repetition rate and central wavelength of about 36.9 MHz and 1550 nm, respectively. The preparation of other optical fields, including the seed injection and local oscillators of HDs, and the realization of mode matching between two OPAs are described in [27]. The technical details for locking the phase of OPA2 and two sets of HDs by loading the feedback signals on PZTs are given in our previous publications (see [27, 30] for details). The transmission efficiency between OPA1 and OPA2 is about 70%. The total detection efficiency of the signal/idler output is about 78%/73%.

## 4. Results

A typical set of data is presented in Fig. 4. The black trace in Fig. 4(a) shows the output spectrum of HD1 when the experimental setup in Fig. 3 is reconfigured as the optimum classical homodyne detection scheme in Fig. 1(a) by setting P1=P2=0. The peak at 1.56 MHz corresponds to the measured power of phase modulation signals. One sees that the SNR is 17.8 ± 0.2 dB, which is the benchmark SNR for the classical phase measurement that we will compare to. Note that the power in all the plots in Fig. 4 is normalized to the shot noise level of HD1 for the sake of easy comparison.

Figure 4(b) shows the result of dual-beam sensing SUI. From the measurement of HD1 and HD2, which are the individual homodyne detections at signal and idler outputs, respectively, one sees that the SNRs of phase signal at 1.56 MHz reads 21.5 ± 0.2 dB and 21.3 ± 0.2 dB. These are 3.7 ± 0.3 dB and 3.5 ± 0.3 dB improvement over the classical measurement result in Fig. 4(a). From the joint measurement of HD1 and HD2 with an optimized electronic gain $k_i = 1$, we find the SNR of measured phase signal is 21.7 ± 0.2 dB, which corresponds to an improvement of 3.9 ± 0.3 dB over the classical result. If the classical limit of the phase measurement were defined the same as that of the single-beam sensing SUI reported in [27, 30], the improvement obtained for the JM case in Fig. 4(b) would be 6.9 dB. This result therefore demonstrates the advantage of dual-beam sensing SUI over the single-beam sensing SUI scheme. Notice that the SNR from joint measurement is slightly higher than those from individual measurement of HD1 or HD2. This is because the gains of OPA1 and OPA2 are finite in our experiment. So the SNRs at each output of SUI are not optimized as described by Eqs. (6) and (7). However, the joint

Optics EXPRESS

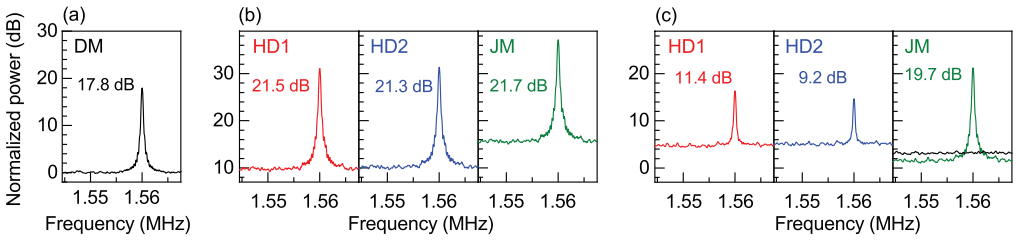


Fig. 4. The spectrums from HD1, HD2 and joint measurement (JM) for the measurement of a phase modulation signal at 1.56 MHz. The noise levels are all normalized to the shot noise level of HD1 at 0 dB. (a) Direct measurement by HD1 with a coherent probe beam when P1 = P2 = 0; (b): Measurement from SUI when P1 = 2mW and P2 = 4mW; (c): Measurement with entangled probe beams (truncated SUI scheme) when P1=2mW and P2=0. The black line in JM of (c) is the shot noise level $SNR_{si}$ of the joint quantity $\Delta i = i_s + k_i i_i$ ($k_i = 1$), which is exactly 3 dB above the shot noise level at 0 dB for individual HD1.

measurement always gives the optimized value (only determined by the entanglement degree) irrespective of the gain of OPA2 .

To measure the information encoded on the entangled state, we implement the dual-beam sensing phase measurement scheme in Fig. 2(c). In this experiment, the experimental setup in Fig. 3 is reconfigured by turning off OPA2 with P2 = 0. During the measurement, P1 and incident seed are the same as those in Fig. 4(b). The results obtained by HD1 and HD2 and JM are presented in Fig. 4(c). Although SNRs extracted from HD1 and HD2 individually are much smaller than the classical measurement result in Fig. 4(a) due to the nature of thermal noise in the individual signal and idler fields, the joint measurement gives an SNR of 19.7 ± 0.2 dB, which is 1.9 ± 0.3 dB better than the SNR in Fig. 4(a). The joint measurement of HD1 and HD2 with $k_i = 1$ has the modulated signal coherently added (nearly 6 dB increase) but noise reduced below joint shot noise level $SNL_{si}$ (see the black line in Fig. 4(c)) due to the anti-correlation on Y quadrature between entangled signal and idler fields [33]. It is interesting to note that had we used the single-beam sensing scheme in [14, 16], the observed SNR would be about 3 dB (factor of 2) smaller and we would have SNR worse (about -1 dB) than the optimum classical method using coherent state as probe.

Moreover, this result also illustrates the loss-tolerant property of SUI. The improvement over the optimum classical scheme for the JM in Fig. 4(c) is only 1.9 dB, which is lower than the 3.9 dB improvement shown in Fig. 4(b). This is because joint measurement of quantum entanglement without amplification is prone to propagation and detection losses (about 25%) in our system. The extra vacuum noise from the loss channels will reduce the effect of quantum correlation and quantum noise reduction. The dual-beam sensing SUI, on the other hand, is insensitive to these losses because each output of OPA2 carries the amplified phase signal and its noise level, lower than a traditional amplifier due to quantum correlated signal and idler inputs, is well above vacuum noise for $G2 \gg G1$. When the vacuum noise is coupled in from the detection loss, both the power of signal and noise will decrease by a similar ratio at the same [34], leading to no obvious change in SNR.

On the other hand, Fig. 4(b) also demonstrates the realization of a quantum optical tap by OPA2. The input fields to OPA2 are the two entangled fields generated from OPA1 (see Fig. 2(c) and Fig. 3), which serve as the quantum signal to be split. The direct joint measurement of phase signal carried by entangled signal and idler beams gives an SNR of 19.7 ± 0.2 dB, as shown in Fig. 4(c), which is 1.9 ± 0.3 dB better than the SNR obtained by classical phase measurement in Fig. 4(a) due to noise reduction originated from the quantum correlation of two entangled fields. However, as we mentioned in theory part, the direct joint measurement scheme

Optics EXPRESS

is sensitive to losses in transmission and detection. After correcting these losses, the SNR of phase signal encoded on the signal and idler entangled fields is deduced to be 22.9 ± 0.2 dB. So we take SNR of input quantum signal as $SNR_{in} = 22.9 \pm 0.2$ dB, while the split fields are the signal and idler outputs of OPA2, which are respectively measured by HD1, HD2. From the result acquired by HD1 and HD2 shown in Fig. 4(c), we find the SNRs of two outputs are $SNR_s = 21.5 \pm 0.2$ dB and $SNR_i = 21.3 \pm 0.2$ dB, respectively. These results lead to transfer coefficients of $T_s = SNR_s/SNR_{in} = 0.72 \pm 0.06$ and $T_i = SNR_i/SNR_{in} = 0.69 \pm 0.06$, with $T_s + T_i = 1.41 \pm 0.09$, which is larger than the classical limit of 1. There are two reasons that deviate the transfer coefficients $T_s$ and $T_i$ from the ideal result $T_s = T_i = 1$ (see Eq. (12)). One is the finite gain of OPA2, the other is the transmission loss and mode mismatching loss occurred when the entangled signal and idler beams are coupled into OPA2.

## 5. Summary and discussion

In summary, we construct a dual-beam sensing SUI and demonstrate its advantages in both phase detection sensitivity and loss tolerance. The measurement results show that SNR is 3.9 ± 0.3 dB higher than that obtained by the optimum classical counterpart in phase measurement. Using the dual-beam sensing SUI, we also realize for the first time the quantum information splitting for phase signal encoded on two entangled fields with transfer coefficients of $T_s + T_i = 1.41 > 1$, satisfying the condition for quantum optical tapping. Compared to previous methods, dual-beam sensing SUI not only makes full use of the quantum resource for phase measurement, but also is insensitive to propagation and detection losses and thus lifts the barrier for the quantum enhanced metrology and quantum communication in practical applications. The loss tolerance property shows that dual-beam sensing SUI has great potential in those situations where quantum efficiency of detection system limits the implementation of quantum enhanced measurement, such as those working at wavelength that lacks efficient photo-detectors (for example, wavelength longer than 2 $\mu$m or ultra violet region).

It is interesting to note that the increase in the sensitivity of phase measurement is the result of quantum resource distribution between two conjugate observables [24]. Under the high gain condition of $G_2, G_1 \gg 1$, all the quantum resource is devoted to phase measurement. However, for the finite gain of $G_1$ but $G_2 \to \infty$ for optimum operation, we find from Eqs. (1) and (7) that the enhancement factor is $2(G_1 + g_1)^4/(G_1^2 + g_1^2)$, which is smaller than the full enhancement factor of $(G_1 + g_1)^2$. This is because, for finite $G_1$, the SNR of amplitude measurement at HD2 is actually non-zero. It can be shown [24] that for amplitude modulation $\epsilon$ and the measurement of $\hat{X} = \hat{a} + \hat{a}^\dagger$ by HD2, we have

$$SNR_{HD2}^{(op)}(AM) = 2I_{ps}\epsilon^2/(G_1^2 + g_1^2). \tag{13}$$

Together with Eq. (7) for phase measurement, we find with $\delta = \epsilon$

$$SNR_{HD1}^{(op)}(PM) + SNR_{HD1}^{(op)}(AM) = 4(G_1 + g_1)^2 I_{ps}\delta^2. \tag{14}$$

So, the sum of the enhancement factors for simultaneous phase and amplitude is conserved and equals to $(G_1 + g_1)^2$. Here, we once again demonstrate the principle of quantum resource sharing between the measurement of conjugate variables even in the non-ideal case of finite gain of $G_1$.

Although the dual-beam sensing scheme has twice the SNR as the single-beam sensing scheme, its implementation requires the frequency and propagation path of two correlated beams to be nearly the same so as to probe the same phase change. Very often SUI is realized with different types of quantum states as in the atom-light hybrid interferometer [32] where the phases involved belong to light and atom separately. In this case the dual beam scheme wouldn't work.

Optics EXPRESS

## Funding

National Natural Science Foundation of China (91836302, 91736105, 11527808, 11874279); National Key Research and Development Program of China (2016YFA0301403).

## References

1. A. A. Michelson and E. W. Morley, "On the relative motion of the earth and of the luminiferous ether," Am. J. Sci. **34**, 333 (1887).
2. C. M. Caves, "Quantum-mechanical noise in an interferometer," Phys. Rev. D **23**, 1693–1708 (1981).
3. V. Giovannetti, S. Lloyd, and L. Maccone, "Quantum metrology," Phys. Rev. Lett. **96**, 010401 (2006).
4. M. Xiao, L.-A. Wu, and H. J. Kimble, "Precision measurement beyond the shot-noise limit," Phys. Rev. Lett. **59**, 278–281 (1987).
5. P. Grangier, R. E. Slusher, B. Yurke, and A. Laporta, "Squeezed-light enhanced polarization interferometer," Phys. Rev. Lett. **59**, 2153–2156 (1987).
6. S. L. Braunstein and H. J. Kimble, "Dense coding for continuous variables," Phys. Rev. A **61**, 042302 (2000).
7. Y. Ma, H. Miao, B. H. Pang, M. Evans, C. Zhao, J. Harms, R. Schnabel, and Y. Chen, "Proposal for gravitational-wave detection beyond the standard quantum limit through EPR entanglement," Nat. Phys. **13**, 776 (2017).
8. B. Yurke, S. L. McCall, and J. R. Klauder, "SU(2) and SU(1,1) interferometers," Phys. Rev. A **33**, 4033–4054 (1986).
9. W. N. Plick, J. P. Dowling, and G. S. Agarwal, "Coherent-light-boosted, sub-shot noise, quantum interferometry," New J. Phys. **12**, 083014 (2010).
10. J. Jing, C. Liu, Z. Zhou, Z. Y. Ou, and W. Zhang, "Realization of a nonlinear interferometer with parametric amplifiers," Appl. Phys. Lett. **99**, 011110 (2011).
11. Z. Y. Ou, "Enhancement of the phase-measurement sensitivity beyond the standard quantum limit by a nonlinear interferometer," Phys. Rev. A **85**, 023815 (2012).
12. A. M. Marino, N. V. Corzo Trejo, and P. D. Lett, "Effect of losses on the performance of an SU(1,1) interferometer," Phys. Rev. A **86**, 023844 (2012).
13. F. Hudelist, J. Kong, C. Liu, J. Jing, Z. Y. Ou, and W. Zhang, "Quantum metrology with parametric amplifier-based photon correlation interferometers," Nat. Commun. **5**, 3049 (2014).
14. B. E. Anderson, P. Gupta, B. L. Schmittberger, T. Horrom, C. Hermann-Avigliano, K. M. Jones, and P. D. Lett, "Phase sensing beyond the standard quantum limit with a variation on the SU(1,1) interferometer," Optica **4**, 752–756 (2017).
15. M. Manceau, G. Leuchs, F. Khalili, and M. Chekhova, "Detection loss tolerant supersensitive phase measurement with an SU(1,1) interferometer," Phys. Rev. Lett. **119**, 223604 (2017).
16. P. Gupta, B. L. Schmittberger, B. E. Anderson, K. M. Jones, and P. D. Lett, "Optimized phase sensing in a truncated SU(1,1) interferometer," Opt. Express **26**, 391–401 (2018).
17. X. Ma, C. You, S. Adhikari, E. S. Matekole, R. T. Glasser, H. Lee, and J. P. Dowling, "Sub-shot-noise-limited phase estimation via SU(1,1) interferometer with thermal states," Opt. Express **26**, 18492–18504 (2018).
18. S. Adhikari, N. Bhusal, C. You, H. Lee, and J. P. Dowling, "Phase estimation in an SU(1,1) interferometer with displaced squeezed states," OSA Continuum **1**, 438–450 (2018).
19. D. Li, B. T. Gard, Y. Gao, C.-H. Yuan, W. Zhang, H. Lee, and J. P. Dowling, "Phase sensitivity at the Heisenberg limit in an SU(1,1) interferometer via parity detection," Phys. Rev. A **94**, 063840 (2016).
20. D. Li, C.-H. Yuan, Z. Y. Ou, and W. Zhang, "The phase sensitivity of an SU(1,1) interferometer with homodyne detection," New J. Phys. **16**, 073020 (2014).
21. X.-L. Hu, D. Li, L. Q. Chen, K. Zhang, W. Zhang, and C.-H. Yuan, "Phase estimation for an SU(1,1) interferometer in the presence of phase diffusion and photon losses," Phys. Rev. A **98**, 023803 (2018).
22. J. Kong, Z. Y. Ou, and W. Zhang, "Phase-measurement sensitivity beyond the standard quantum limit in an interferometer consisting of a parametric amplifier and a beam splitter," Phys. Rev. A **87**, 023825 (2013).
23. B. E. Anderson, B. L. Schmittberger, P. Gupta, K. M. Jones, and P. D. Lett, "Optimal phase measurements with bright- and vacuum-seeded SU(1,1) interferometers," Phys. Rev. A **95**, 063843 (2017).
24. J. Li, Y. Liu, L. Cui, N. Huo, S. M. Assad, X. Li, and Z. Y. Ou, "Joint measurement of multiple noncommuting parameters," Phys. Rev. A **97**, 052127 (2018).
25. X. Li, Q. Pan, J. Jing, J. Zhang, C. Xie, and K. Peng, "Quantum dense coding exploiting a bright einstein-podolsky-rosen beam," Phys. Rev. Lett. **88**, 047904 (2002).
26. S. Steinlechner, J. Bauchrowitz, M. Meinders, H. MÃijller-Ebhardt, K. Danzmann, and R. Schnabel, "Quantum-dense metrology," Nat. Photonics **7**, 626–630 (2013).
27. Y. Liu, J. Li, L. Cui, N. Huo, S. M. Assad, X. Li, and Z. Y. Ou, "Loss-tolerant quantum dense metrology with SU(1,1) interferometer," Opt. Express **26**, 27705–27715 (2018).
28. B. Abbott, R. Abbott, R. Adhikari, P. Ajith, B. Allen, G. Allen, R. Amin, S. Anderson, W. Anderson, M. Arain *et al.*, "Ligo: the laser interferometer gravitational-wave observatory," Reports Prog. Phys. **72**, 076901 (2009).
29. R. L. Forward, "Wideband laser-interferometer graviational-radiation experiment," Phys. Rev. D **17**, 379–390 (1978).
30. X. Guo, X. Li, N. Liu, and Z. Y. Ou, "Quantum information tapping using a fiber optical parametric amplifier with noise figure improved by correlated inputs," Sci. Rep. **6**, 30214 (2016).

Optics EXPRESS


31. R. Tang, J. Lasri, P. S. Devgan, V. Grigoryan, P. Kumar, and M. Vasilyev, "Gain characteristics of a frequency nondegenerate phase-sensitive fiber-optic parametric amplifier with phase self-stabilized input," Opt. Express **13**, 10483 (2005).
32. B. Chen, C. Qiu, S. Chen, J. Guo, L. Chen, Z. Ou, and W. Zhang, "Atom-light hybrid interferometer," Phys. Rev. Lett. **115**, 043602 (2015).
33. X. Guo, N. Liu, Y. Liu, X. Li, and Z. Y. Ou, "Generation of continuous variable quantum entanglement using a fiber optical parametric amplifier," Opt. Lett. **41**, 653 (2016).
34. J. Li, Y. Liu, N. Huo, L. Cui, X. Li, and Z. Ou, "Loss-tolerant measurement of continuous-variable quantum entanglement with the aid of a high gain parametric amplifier," arXiv preprint arXiv:1808.10258 (2018).
35. J. H. Shapiro, "Optical waveguide tap with infinitesimal insertion loss," Opt. Lett. **5**, 351–353 (1980).
36. J.-A. Levenson, I. Abram, T. Rivera, P. Fayolle, J. Garreau, and P. Grangier, "Quantum optical cloning amplifier," Phys. Rev. Lett. **70**, 267 (1993).
37. D. K. Serkland and P. Kumar, "Tunable fiber-optic parametric oscillator," Opt. Lett. **24**, 92 (1999).
38. X. Guo, X. Li, N. Liu, L. Yang, and Z. Y. Ou, "An all-fiber source of pulsed twin beams for quantum communication," Appl. Phys. Lett. **101**, 261111 (2012).